International Conferences on Recent Advances in Geotechnical Earthquake Engineering and Soil Dynamics

1981 - First International Conference on Recent Advances in Geotechnical Earthquake Engineering & Soil Dynamics

27 Apr 1981, 2:00 pm - 5:00 pm

Analysis of Stress Distribution in Torsional Shear Testing

J. S. DeNatale
University of California, Davis, CA

C. K. Shen
University of California, Davis, CA

L. R. Herrmann
University of California, Davis, CA

J. L. Vrymoed
California Department of Water Resources, California

Proceedings: First International Conference on Recent Advances in Geotechnical Earthquake Engineering and Soil Dynamics, April 26 - May 3, 1981, St. Louis, Missouri

Analysis of Stress Distribution in Torsional Shear Testing

J. S. DeNatale, Associate, C. K. Shen, Professor, L. R. Herrmann, Professor
University of California, Davis

J. L. Vrymoed
Associate Engineer, California Department of Water Resources

SYNOPSIS The research described herein is concerned with the establishment of a specimen geometry that will lead to a more uniform stress distribution in cyclic torsional shear testing. This goal is realized by means of a parametric study using the method of finite elements and a homogeneous, isotropic, linear-elastic soil characterization. The results of these analyses provide a good qualitative measure of the relative effects of the several parameters under consideration. On the basis of the parametric study, design charts are developed which enable an appropriate specimen geometry to be selected for any specified degree of stress uniformity.

INTRODUCTION

The use of torsional shear testing to determine the seismic response of soils has been reported by a number of researchers, including Ishibashi et al. (1974), Ishihara et al. (1972,1975), and Iwasaki et al. (1978). The principal benefit that may be derived from this type of testing lies in the fact that the technique enables a soil specimen to be subjected to a wide variety of combined stress states. In this manner it becomes possible to more closely simulate the actual field stress and strain states induced by earthquake loading. However, a number of researchers, including Ladd and Silver (1975), Yoshimi and Oh-oka (1975), Wright et al. (1978), and DeNatale (1979), have shown that the boundary conditions and specimen geometries associated with these devices fail to ensure that a high degree of stress and strain uniformity will exist within the soil sample throughout the entire loading sequence.

The research to be described herein is concerned with the establishment of a specimen geometry that will lead to a more uniform stress distribution in cyclic torsional shear testing. This goal is realized by means of a parametric study using the method of finite elements, in which the soil is characterized as a homogeneous, isotropic, linear-elastic material. A total of 24 different combinations of parameters are considered. The subsequent finite element analyses reveal the relations between the magnitude and the uniformity of the stress distribution and such parameters as (i) the height-to-diameter ratio h/d, (ii) the inner-to-outer radius ratio r_i/r_o, (iii) the wall thickness r_o-r_i, (iv) the applied confining stress-to-axial stress ratio σ_3/σ_1, (v) the magnitude of the applied torsional shearing strain $\gamma_{z\theta}$, and (vi) the Poisson's ratio of the soil ν. In order that the stress distributions at various stages in the cyclic loading sequence could be compared, the response of the soil specimen was characterized in terms of the octahedral shear stress τ_{oct}. Although the assumption of linear-elasticity is an oversimplification of real soil behavior, these analyses nevertheless provide a good qualitative measure of the relative effects of the several parameters under investigation.

On the basis of the parametric study, a method is proposed whereby design charts may be developed which enable an appropriate specimen geometry to be selected for any specified degree of stress uniformity required during the torsional shear testing.

THE FINITE ELEMENT MODEL

The analyses were preformed using the finite element program NAAS developed by Herrmann (1968). The program uses four-node isoparametric quadrilateral elements, and has the capability of treating both two- and three-dimensional elasticity problems.

The complete boundary conditions and a typical finite element mesh are show in Figure 1. It should be noted that because the hollow cylindrical system has two axes of symmetry (axes r and z in Figure 1), it was only necessary to analyze one quadrant of a given vertical cross-section.

In order to closely simulate the procedure that is actually followed in the laboratory, the analytical loading was applied in two stages. Initially, in order to simulate the radial confining stress σ_3, a uniform horizontal stress σ_r was applied to the exterior (and, for the case of hollow configurations, interior) lateral surface of the finite element model. Next, in order to simulate the axial stress σ_1 that is applied to the rigid upper loading platen during the triaxial stage of the loading sequence, a uniform vertical displacement $u_z = \delta$ was applied to the upper boundary of the finite element idealization. In addition, since torsional shear testing requires that there be no slippage between the soil specimen and the loading platens, no radial displacement was permitted along the upper surface of the analytical model ($u_r=0$). Finally, in order to simulate the rotational shearing strain that is imparted to the soil specimen during the torsional shear stage of the loading sequence, a tangential displacement $u_\theta = \phi\, r$ (where ϕ = the angle of twist $= \gamma_{\theta z}\, h/r$) was applied to the upper surface of the finite element idealization.

PARAMETERS UNDER INVESTIGATION

A total of 24 cases were analyzed using different combinations of specimen geometry (h/d, r_i/r_o, and r_o-r_i), boundary loadings (σ_3/σ_1 and $\gamma_{z\theta}$), and material properties (ν). A complete summary of the various cases is presented in Table I.

For each of the 24 cases listed in Table I, finite element solutions were generated for each of six distinct levels of

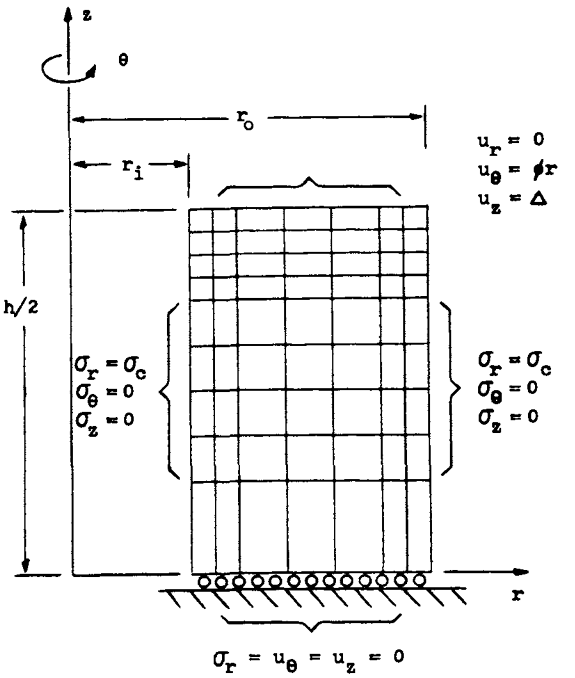

Figure 1. **The Applied Boundary Conditions and a Typical Finite Element Mesh.**

Case Number	h/d	r_i/r_o	σ_1 (psi)	σ_3 (psi)	E (psi)	ν	Torsion Levels
1	1	0.00/1.50	40	0	7500	0.333	1 - 6
2	1	0.00/1.50	40	10	7500	0.333	1 - 6
3	2	0.00/1.50	40	0	7500	0.333	1 - 6
4	2	0.00/1.50	40	10	7500	0.333	1 - 6
5	2	0.00/1.50	40	20	7500	0.333	1 - 6
6	2	0.00/1.50	40	40	7500	0.333	1 - 6
7	4	0.00/1.50	40	0	7500	0.333	1 - 6
8	4	0.00/1.50	40	10	7500	0.333	1 - 6
9	2	0.50/1.50	40	0	7500	0.333	1 - 6
10	2	0.50/1.50	40	10	7500	0.333	1 - 6
11	2	0.50/1.50	40	20	7500	0.333	1 - 6
12	2	0.50/1.50	40	40	7500	0.333	1 - 6
13	2	1.00/1.50	40	0	7500	0.333	1 - 6
14	2	1.00/1.50	40	10	7500	0.333	1 - 6
15	2	1.00/1.50	40	20	7500	0.333	1 - 6
16	2	1.00/1.50	40	40	7500	0.333	1 - 6
17	2	1.25/1.50	40	0	7500	0.333	1 - 6
18	2	1.25/1.50	40	10	7500	0.333	1 - 6
19	2	1.25/1.50	40	20	7500	0.333	1 - 6
20	2	1.25/1.50	40	40	7500	0.333	1 - 6
21	2	0.50/1.50	40	0	7500	0.400	1 - 6
22	2	0.50/1.50	40	10	7500	0.400	1 - 6
23	2	0.50/1.50	40	20	7500	0.400	1 - 6
24	2	0.50/1.50	40	40	7500	0.400	1 - 6

Table I. **Combinations of Parameters Considered in the Finite Element Study.**

applied torsional shear. These six levels are defined in Table II. It was desired to have the six torsion levels span the entire range of the combined loading sequence. In other words, it was desired to examine a range of stress distributions wherein, at the lower bound, the overall stress uniformity was dominated by the effects of the triaxial stage of the loading (and thus $\tau_{rz} \ggg \tau_{z\theta}$), whereas, at the upper bound, the overall stress uniformity was dominated by the effects of the torsional shear stage of the loading (and thus $\tau_{rz} \lll \tau_{z\theta}$).

In order that the shear stress distributions at various stages in the combined loading sequence could be directly compared, the response of the specimen was characterized in terms of the octahedral shear stress τ_{oct}. Octahedral stresses and strains have often been used as the basis for non-linear material characterizations, and may also be related to such failure criteria as the Mises yield criterion (DeNatale, 1979). The degree of stress uniformity was then defined by considering the percentage of the specimen (by volume) having an octahedral shear stress within some given percentage of the mean (or average) value, $\bar{\tau}_{oct}$.

Torsion Level	1	2	3	4	5	6
$(\gamma_{z\theta})_{max}$	0.00%	0.09%	0.18%	0.90%	1.80%	9.00%

Table II. **Relation Between Torsion Level and Applied Shearing Strain.**

RESULTS OF THE LINEAR-ELASTIC ANALYSES

A sampling of the results of the parametric computer study is presented in Tables III and IV. As may be observed, the study has revealed a number of interesting relations between the various parameters under consideration and the uniformity of the octahedral shear stress in the finite element model. The most significant of these trends may be summarized as follows:

a) the distribution of τ_{oct} remains qualitatively about the same, regardless of h/d or r_i/r_o, and provided that there is no applied torsion;
b) under triaxial loading alone, the greatest shear stress non-uniformity is always in the vicinity of the specimen-platen interface;
c) under triaxial loading alone, the uniformity of the octahedral shear stress distribution increases with increasing h/d and increasing r_i/r_o;
d) the loading conditions which result in the radial normal strain ϵ_r being zero (namely, $\sigma_3/\sigma_1 = \nu/(1-\nu)$ by Hooke's Law) result in a complete uniformity of τ_{oct}, provided that there is no applied torsion;
e) if the shear stress distribution is examined in terms of relative deviations from the mean, the greatest non-uniformity occurs whenever a hydrostatic loading is applied (that is, $\sigma_1 = \sigma_3$). However, under this loading condition the absolute deviations from the mean are quite small;
f) under torsional loading, the uniformity of the octahedral shear stress distribution increases with increasing r_i/r_o and decreasing (r_o-r_i);

Case Number	σ_1 (psi)	σ_3 (psi)	h/d	r_i/r_o	% of specimen (by volume) having a τ_{oct} within 5% of $\bar{\tau}_{oct}$ Torsion Level 1	Torsion Level 2	Torsion Level 3	Torsion Level 4	Torsion Level 5	Torsion Level 6
1	40	0	1	0.00/1.50	41%	41%	39%	16%	20%	13%
3	40	0	2	0.00/1.50	57%	58%	62%	61%	17%	13%
7	40	0	4	0.00/1.50	88%	88%	89%	58%	27%	13%
9	40	0	2	0.50/1.50	73%	73%	75%	69%	23%	0%
13	40	0	2	1.00/1.50	76%	78%	81%	81%	53%	20%
17	40	0	2	1.25/1.50	78%	78%	80%	92%	85%	60%
2	40	10	1	0.00/1.50	49%	49%	48%	36%	17%	13%
4	40	10	2	0.00/1.50	83%	84%	85%	51%	15%	13%
8	40	10	4	0.00/1.50	92%	93%	93%	50%	15%	13%
10	40	10	2	0.50/1.50	86%	87%	87%	62%	20%	0%
14	40	10	2	1.00/1.50	90%	90%	92%	81%	54%	20%
18	40	10	2	1.25/1.50	91%	91%	91%	94%	85%	60%

Table III. Influence of σ_3/σ_1, h/d, r_i/r_o, and $(\gamma_{z\theta})_{max}$ on the Uniformity of the Octahedral Shear Stress.

g) if the ratio of σ_3/σ_1 which results in complete uniformity is denoted by $(\sigma_3/\sigma_1)^*$, then as the difference between $(\sigma_3/\sigma_1)^*$ and the actual value of σ_3/σ_1 increases, the degree of shear stress uniformity steadily decreases;

h) the magnitude of σ_3/σ_1, at which complete uniformity occurs increases as the value of Poisson's ratio is increased.

Since the nonlinearities which characterize the behavior of most real soils have not been included in the finite element model, and since the choice of parameter values is, of necessity, somewhat arbitrary, the numerical results should be interpreted with caution. Nonetheless, the numerous trends which have just been mentioned should provide a useful insight into the features that are needed to guarantee a uniform distribution of stress and strain in cyclic torsional shear testing.

A typical design chart is shown in Figure 2. This particular chart was developed for the case of h/d = 2, and allows one to select the appropiate inner-to-outer radius ratio r_i/r_o, when it has been specified that a given percentage of the specimen must have an octahedral shear stress within ξ_2 = 5% of the mean value, $\bar{\tau}_{oct}$. Additional design charts, as well as several examples which illustrate their use, are provided by DeNatale (1979). It should be pointed out that, due to the assumption of linear elasticity, the design charts would be most accurate for low levels of torsional shear (say torsion levels #1 through #4, wherein $(\gamma_{z\theta})_{max}$ is less than 1%). Although design curves have also been generated for higher levels of torsional shear (curves #5 and #6 in Figure 2), the validity of these curves is questionable, since the soil response under these loading conditions may be quite non-linear.

FORMULATION OF DESIGN CHARTS

In order to establish an appropriate specimen geometry for use in cyclic torsional shear testing, it becomes necessary to quantify the various qualitative relations summarized above. The statistical data that was generated during the linear-elastic finite element analyses (such as that contained in Tables III and IV) permit this extension to be made. On the basis of the statistical results, design charts may be developed which relate the degree of stress uniformity in a test sample to its geometrical properties (that is h/d, r_i/r_o, and r_o-r_i). Using these design charts, one may readily select an appropriate specimen geometry for any given required degree of stress uniformity.

CONCLUSION

The finite element analyses that have been carried out during the present investigation have established a number of qualitative relationships between the degree of stress uniformity and such parameters as (i) the height-to-diameter ratio, (ii) the inner-to-outer radius ratio r_i/r_o, (iii) the wall thickness r_o-r_i, (iv) the applied confining stress-to-axial stress ratio σ_3/σ_1, (v) the magnitude of the applied torsional shearing strain $\gamma_{z\theta}$, and (vi) the Poisson's ratio of the soil ν. Although an isotropic, linear-elastic soil characterization was assumed, these qualitative relations should be valid for most, if not all, real soils.

σ_1 (psi)	σ_3 (psi)	% of specimen (by volume) having a τ_{oct} within 5% of $\bar{\tau}_{oct}$ $\nu = 0.333$	$\nu = 0.400$
40	0	73%	53%
40	10	86%	68%
40	20	100%	86%
40	40	0%	7%

Table IV. Influence of σ_3/σ_1 and Poisson's ratio ν on the Uniformity of the Octahedral Shear Stress.

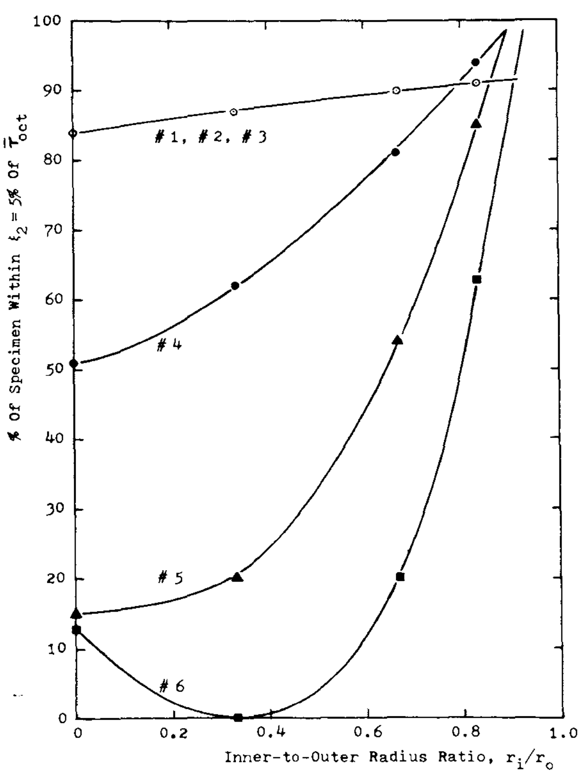

Figure 2. Relation Between Stress Uniformity and r_i/r_o for Levels #1 - #6 of Applied Torsional Shear.

In order to enable a specific sample geometry to be selected for any given required degree of stress uniformity, design charts have been developed which are consistent with the results of the computer analyses. However, because these charts by necessity tend to quantify are aforementioned relations, they are of limited validity. In most cyclic torsional shear testing the maximum shear strain is kept quite small (say, less than 1%), and the assumption of linear-elasticity is reasonable. Hence, for these low levels of torsional shear the design charts are likely to be quite dependable. However, for higher levels of torsional shear (such as torsion levels #5 and #6, wherein $(\gamma_{z\theta})_{max}$ is greater than 1%) the soil response may be quite non-linear, in which case the quantitative results of the finite element analyses, and thus the design charts, may not be exactly correct. Hence, it should once again be pointed out that the method by which these charts are developed is of much greater significance than their specific content.

ACKNOWLEDGEMENT

The authors like to express their gratitude to the State of California Department of Water Resources for sponsoring the research described herein.

REFERENCES

DeNatale, J.S. (1979), "Distribution of Stress And Strain In Combined Triaxial And Torsional Shear Loading," Masters Thesis, University of California, Davis.

Herrmann, L.R. (1968), "Three-Dimensional Elasticity Analysis of Non-Axisymmetrically Loaded Solids of Revolution," University of California, Davis, Department of Civil Engineering, Report No. 68-12-1.

Ishibashi, I., and Sherif, M. (1974), "Liquefaction Of A Loose Saturated Sand By Torsional Simple Shear Device," University of Washington, Soil Engineering Research Report No. 8.

Ishihara, K., and Li, S., (1972), "Liquefaction of Saturated Sand In Triaxial Torsion Shear Test," Soils and Foundation, Vol. 12, No. 2, pp. 19-39.

Ishihara, K., and Yasuda, S., (1975), "Sand Liquefaction In Hollow Cylinder Torsion Under Irregular Excitation," Soils and Foundations, Vol. 15, No. 1, pp. 45-59.

Iwasaki, T. et al (1978), "Shear Moduli of Sands Under Cyclic Torsional Shear Loading", Soils and Foundations, Vol. 18, No. 1, pp. 39-56.

Ladd, R., and Silver, M., (1975), Discussion of "Soil Liquefaction By Torsional Simple Shear Device," Journal A.S.C.E. Geotechnical Engineering Division, Vol. 101, No. GT8, pp. 827-829.

Wright, D. et al (1978), "Shear Devices for Determining Dynamic Soil Properties," Proceedings, A.S.C.E. Conference on Earthquake Engineering and Soil Dynamics, Vol. 1, pp. 1056-1075.

Yoshimi, Y., and Oh-oka, H., (1975), "Influence of Degree of Shear Stress Reversal on the Liquefaction Potential of a Saturated Sand," Soils and Foundations, Vol. 15, No. 3, pp. 27-40.